

中国激光

利用原子吸收谱线实现气室温控

吴丽珍^{1,2}, 祝孝杰^{1,2}, 蒋双辉^{1,2}, 田原¹, 张奕^{1**}, 陈杰华^{1*}, 顾思洪¹

¹中国科学院精密测量科学与技术创新研究院原子频标重点实验室, 湖北 武汉 430074;

²中国科学院大学物理学院, 北京 100049

摘要 要实现微型光学原子磁强计需要精确测定气室温度和实现高精度气室温控。提出了一种无温度传感器的气室温控方案。该方案首先探测激光输出功率,采用激光功率伺服控制激光器的注入电流以锁定光功率;然后探测原子吸收光谱,利用同步调制解调技术将其转变成激光频率鉴频信号,采用激光频率伺服控制激光器温度,将激光频率锁定在吸收谱线中心;最后利用原子吸收光谱中心信号幅度来测量气室温度,从而实现气室温控。采用本方案实现了气室温控,温控效果与采用热敏电阻测温所实现的气室温控效果相当,为实现微型光学原子磁强计气室温控提供了一种备选方案。

关键词 激光光学; 微型光学原子磁强计; 气室温控; 原子吸收谱线; 激光稳频

中图分类号 O433.1 文献标志码 A

DOI: 10.3788/CJL221493

1 引言

光学原子磁强计利用光与原子作用所产生的光谱来测量磁场,是目前灵敏度最高的磁强计之一^[1]。除可实现高灵敏度外,利用微加工技术,其探头还可实现微型化,从而制成微型光学原子磁强计^[2]。微型光学原子磁强计体积小、功耗低、灵敏度高,在地质勘探^[3]、地磁导航^[4]、水下目标探测^[5]等具有广阔应用前景。

要实现高灵敏度微型光学原子磁强计,一般要实现高精度气室温控以产生合适密度的原子蒸气,因此要精确测量气室温度。一种经典测温方案是采用温度传感器,如铂电阻,来测量气室温度^[6]。中国原子能科学研究院徐昆等^[7]采用加热丝在不同温度下阻值率不同的原理来测量气室温度,方案结构简单。然而,实现这两个方案需要挑选或定制无磁器件,且测量的是气室外部温度,测量结果易受环境影响。Castro 等^[8]提出利用红外传感器实现测温,具有非接触优点。刘帅等^[9]提出光纤光栅准分布式高温传感器,利用温度改变导致的波长漂移来测量温度。王卓等^[10]提出利用不同气室温度引起的光折射率变化来实现气室温度测量。但这些方案装置难以小型化,因此难以用于微型光学原子磁强计研制。

本文介绍了一种气室测温及控温方案。采用激光作为光源,锁定激光功率后,利用碱金属气室对线偏振激光的吸收谱线作为参考,将激光频率锁定在谱线中心频率处,通过探测原子对共振激光的吸收率来测量

气室温度,从而实现气室温控。本方案无需温度传感器,器件易于微型化,适用于微型光学原子磁强计研制。

2 方法与实验装置

微型光学原子磁强计常采用气室中碱金属原子蒸气与激光作用,从而获得原子谱线。气室中碱金属原子蒸气密度与温度的关系可以表示为 $n = 10^{21.886 + A - B/T} / T^{11}$, 其中, n 为原子蒸气密度, 单位为 cm^{-3} , T 为气室温度, 单位为 K, A 和 B 是与碱金属原子相关的常数, 对于本文实验中所采用的液态⁸⁷Rb 原子, $A=4.312, B=4040$ 。单色线偏振光经过气室后的透射率可表示为 $I_z/I_0 = K_0 \exp[-n\sigma(v)L]$, 其中, I_z 为出射激光强度, I_0 为入射激光强度, K_0 为气室壁导致的衰减率, L 为光在气室内的传播距离, $\sigma(v)$ 为原子对频率为 v 的光子的吸收截面, $\sigma(v) = k \int_0^\infty L(v-v')G(v'-v_0)dv'$, k 为常数, $L(v-v') = \frac{\Gamma_L/(2\pi)}{(v-v'-v_0)^2 + (\Gamma_L/2)^2}$, Γ_L 为碱金属原子与缓冲气体分子碰撞导致的压力展宽, v_0 为吸收谱线中心频率, $G(v'-v_0) = \frac{2\sqrt{\ln 2}}{\Gamma_G} \exp\left[-4\frac{(v'-v_0)^2}{\Gamma_G^2} \ln 2\right]$, Γ_G 为碱金属原子热运动导致的多普勒展宽。温度变化会导致压力展宽 Γ_L 和多普勒展宽 Γ_G 变化, 但比原子蒸气密度的变化

收稿日期: 2022-12-05; 修回日期: 2022-12-28; 录用日期: 2023-02-08; 网络首发日期: 2023-03-09

基金项目: 国家重点研发计划(2018YFB2002400)

通信作者: *andychen@apm.ac.cn; **zhangyi@apm.ac.cn

率小得多。假设 Γ_L 和 Γ_G 为常数,且激光频率为吸收谱线中心频率,即 $v = v_0$,则有

$$I_z/I_0 = K_0 \exp \left[-10^{21.886 + A - B/T} \sigma(v_0) L/T \right], \quad (1)$$

$$\text{式中: } \sigma(v_0) = k \frac{\Gamma_L^2}{\Gamma_G} \left[1 - \operatorname{erf} \left(\frac{\sqrt{\ln 2} \Gamma_L}{\Gamma_G} \right) \right], \text{ 其中 } \operatorname{erf}(\cdot)$$

为误差函数。由式(1)可见:我们锁定入射激光强度并将激光频率锁定在谱线中心频率后,透过气室的光强度只与温度 T 有关,通过探测透射光强度就可测量气室温度,从而实现气室温控。

我们利用此方法开展了实验研究。实验中激光和气室温度控制由配有模拟输入输出采集卡的计算机完成,所采用的实验装置如图 1 所示。光源为集成半导体制冷器(TEC)和热敏电阻的垂直腔面发射激光器(VCSEL),可通过温控仪控温。将电流源输出的直流电流注入到 VCSEL 中产生平行传播的激光。激光经过偏振片后再经过半波片(HWP)和偏振分束器(PBS)分为两束。一束被光电探测放大器(PDA)1 探测并转换成电压信号,经激光功率伺服模块转变成 VCSEL 注入电流的负反馈信号,叠加在 VCSEL 注入电流上,从而实现激光功率锁定。另一束进入气室与 ^{87}Rb 原子作用。气室内除充有 ^{87}Rb 元素外还充入

10 kPa 氮气,实验中气室工作温度约为 65 °C,压力增宽约为 1.2 GHz,多普勒增宽约为 0.6 GHz,因此 D1 线基态超精细能级可分辨,而激发态超精细能级不可分辨。激光与铷 87 原子 D1 线作用,产生原子吸收谱线。透射光被 PDA2 探测并转变成电压信号。为了将原子吸收谱线转变成激光频率鉴频信号,锁相放大器产生交流电流均方根值为 200 nA、交流电流频率为 100 kHz 的正弦信号,通过 T 型偏置器(bias-T)将该信号叠加在电流源产生的直流电流上,利用同步解调从 PDA2 输出电压信号中提取出微分形式吸收谱线,其经过激光频率伺服模块转变成 TEC 驱动电流的负反馈信号,叠加在 TEC 驱动电流上,将激光频率锁定在吸收谱线中心。

气室置于无磁性的陶瓷外壳中,信号发生器产生交流电流驱动外壳上的加热丝实施整体加热。PDA2 输出的电压信号经过比例积分微分(PID)1 模块后转变成加热功率控制信号,控制信号发生器输出功率,实现气室温控。为评估本文提出方案的控温效果,气室两侧设有两个紧贴气室的热敏电阻,热敏电阻 1 测量原子气室温度,用于 PID2 实现基于热敏电阻测温的气室温控;热敏电阻 2 监测气室温度,用于比较两种温控方式的温控效果。激光功率伺服、激光频率伺服及 PID1 和 PID2 模块功能均由计算机完成。

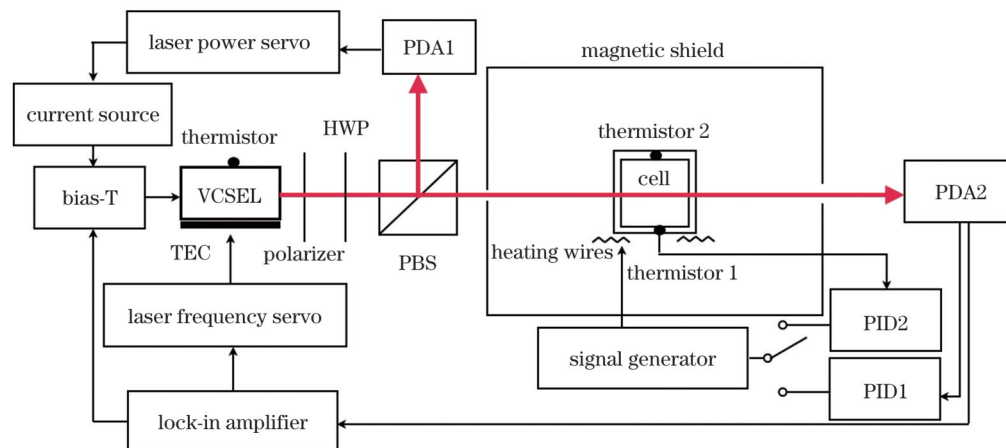


图 1 实验装置示意图
Fig. 1 Schematic of experimental devices

3 结果与讨论

3.1 VCSEL 功率和频率锁定效果

实验所用 VCSEL 在注入电流约为 1.2 mA、温度约为 20 °C 时的输出激光频率处于吸收谱线附近。为获得该 VCSEL 在工作温度处的输出激光功率随注入电流的变化特征以进行激光功率伺服控制,我们利用温控仪将 VCSEL 温度控制为 20 °C,在 1.1~1.3 mA 区间以 50 nA 为间隔调节 VCSEL 注入电流,记录 PDA1 输出电压平均幅度,获得注入电流与 PDA1 输出的关系,通过线性拟合获得 PDA1 输出电压随 VCSEL 注入

电流变化的斜率(S_p)。实施伺服控制时,计算机程序以 0.2 s 为周期测量 PDA1 输出,与设定光功率对应电压值作差,除以 $-S_p$ 后叠加在原注入电流上,从而锁定 VCSEL 输出功率。锁定激光功率后,监测 VCSEL 注入电流变化,测得变化的峰峰值约为 33 nA,测量获得的 VCSEL 输出频率和电流的比值为 305 GHz/mA,计算对应的频率变化峰峰值为 10 MHz 左右,VCSEL 输出激光线宽约为 100 MHz,因此激光功率锁定环路不会显著增加激光频率抖动。

为获得该 VCSEL 在工作电流处的输出激光频率随 TEC 驱动电流的变化特征,我们将气室温度加热到

工作温度 65 ℃附近,将 VCSEL 注入电流设为 1.2 mA, 调节 TEC 驱动电流使激光器温度在 20 ℃附近, 在所需驱动电流±0.1 mA 区间内以 0.01 mA 为间隔调节 TEC 驱动电流, 获得 TEC 驱动电流与锁相放大器输出的关系, 通过线性拟合获得吸收谱线过零点附近锁相放大器输出电压随驱动 TEC 电流变化的斜率(S_i)。计算机程序以 50 ms 为周期测量锁相放大器输出, 除以 $-S_i$ 后叠加在原 TEC 驱动电流上, 将 VCSEL 输出频率锁定在谱线中心频率处。实验中我们将气室温度设定为工作温度完成了激光频率锁定, 当气室温度远离工作温度时, 斜率 S_i 会发生变化, 但激光频率锁定仍可实现。

在实施激光功率锁定前后和在实施激光频率锁定前后, 我们利用计算机记录 PDA1 输出, 并进行快速傅里叶变换, 计算激光相对强度噪声。不同情况下获得的相对强度噪声功率谱密度的开方结果如图 2 所示。其中, 实线为固定 VCSEL 注入电流、固定 TEC 驱动电流情况下的噪声谱, 虚线为固定 TEC 驱动电流、激光功率锁定情况下的噪声谱, 点划线为激光功率锁定和频率锁定情况下的噪声谱。可以看出: 实现激光功率锁定后, 激光在 4 Hz 以下的相对强度噪声显著减小; 实现激光频率锁定后, 激光在 0.1 Hz 以下的相对强度噪声进一步减小。

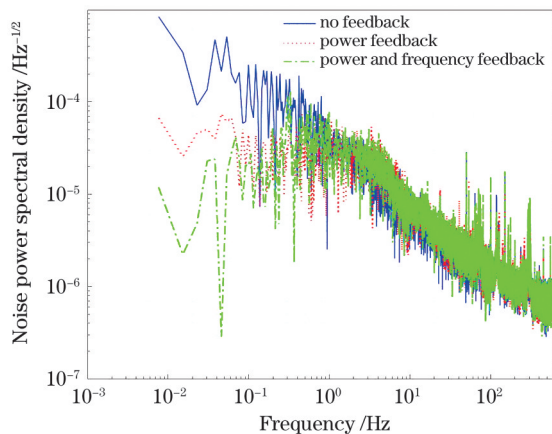


图 2 采样频率为 1000 Hz、记录数据时间为 210 s 时的归一化噪声功率谱

Fig. 2 Normalized noise power spectra when sampling rate is 1000 Hz and data recording time is 210 s

3.2 气室温度控制效果

在实现激光功率和频率锁定后, 我们利用热敏电阻 1 测量气室温度, 并实施气室温控, 在 55.6~75.0 ℃区间改变气室温度, 记录 PDA2 输出信号。通过平均滤波滤除光电信号中的高频噪声, 从而减小高频光噪声对测温的影响。获得的 PDA2 输出与气室温度的关系如图 3 所示。可以看出: PDA2 输出随气室温度显著变化, 在 63~67 ℃区间, 变化斜率较大, 此为较佳的测控温度范围。实验中, 我们将原子气室温度控制在 65 ℃左右。利用式(1), 我们获得了拟合曲线。在 61~75 ℃范围内, 利用拟合曲线计算气室温度的误差

不大于±0.3 ℃。

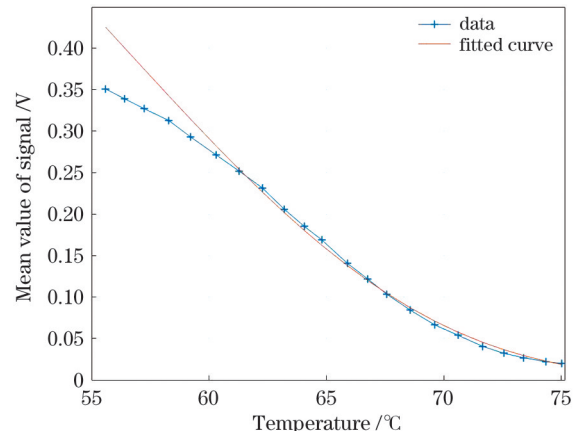


图 3 透射光信号平均值与气室温度关系
Fig. 3 Mean value of transmitted optical signal versus cell temperature

利用前述实验装置, 我们分别利用 PDA2 输出信号幅度和热敏电阻 1 输出阻值, 采用 PID 控制实现了气室温控。在所调的各自最佳 PID 参数下, 我们记录了两种温控方式下热敏电阻 2 的阻值随时间变化的曲线, 并转换成图 4(a)所示的气室温度随时间变化的曲线。根据图 4(a)计算出 Allan 方差^[13], 结果如图 4(b)所示, 可见两种温控方式在不同平均时间下的 Allan 方差相当, 表明温控效果相当。对于我们研制的原子磁强计, 该气室最佳工作温度为 65~70 ℃, 因此在实验中, 我们在 70 ℃开展了温控实验, 所获温控效果基本相当。

3.3 讨论

本文实验中我们采用缓冲气体压强为 10 kPa 的气室, 若采用更大压强缓冲气体气室, 随着吸收谱线变宽, 实现的温控精度会有所下降, 且激光稳频效果会变差, 但采用充有约 80 kPa 氦气的气室和类似方案依然可实现频率漂移为十几 MHz/h 的稳频效果^[14]。

本方案所获激光已实现稳频, 通过分束就可获得用于极化原子的激光, 从而研制原子磁强计。相比采用热敏电阻进行测温, 本方案系统相对复杂, 成本高, 但能够解决温度传感器磁干扰问题。VCSEL 具有体积小、功耗低的优点, 常用于微型光学原子磁强计研制^[15-16]。实验中所用的光学器件和光电二极管也易于微型化, 因此本方案适用于微型光学原子磁强计研制。目前微型光学原子磁强计一般采用温度传感器测量激光器温度, 从而实现温控; 采用频率锁定伺服, 通过控制注入电流, 将激光频率锁定在原子谱线中心。当激光器温度发生变化时, 注入电流会补偿其引起的频率变化, 从而导致激光功率变化。另外, 长期运行老化后, 激光器输出激光功率和波长都会发生单向变化^[17]。这些因素造成原子磁强计长期运行后性能发生变化。本方案在实现气室温控的同时, 锁定了激光器输出激光功率, 通过对激光器输出激光进行分光就能获得激光功

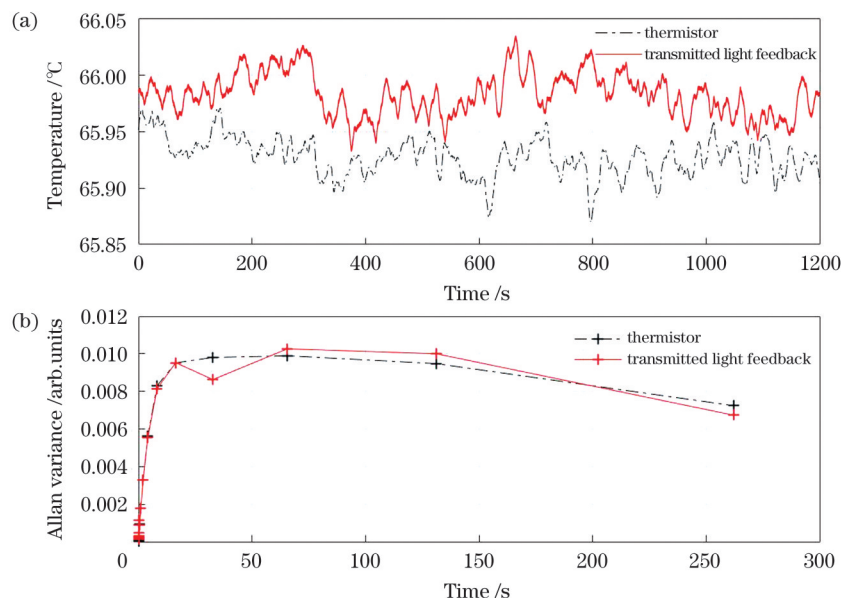


图4 采样频率为1000 Hz时利用热敏电阻和透射光信号实现气室温度控制的效果。(a)气室温度随时间变化的曲线;(b)Allan方差
Fig. 4 Temperature control effects of cell using thermistor and transmitted light signal when sampling frequency is 1000 Hz. (a) Cell temperature versus time; (b) Allan variance

率和频率均锁定的光束,应用于原子磁强计时可减小磁强计温度敏感性和长期工作后性能恶化的程度。

4 结 论

提出利用原子对共振光的吸收光谱实现气室温度测量和温控的方案。在实验上实现了激光功率和频率锁定以及气室温控。实现激光功率和频率锁定后,激光强度噪声相比自由运行状态显著减小。采用热敏电阻测量气室温度,从而实现了气室温控。采用所提方案得到的温控效果与采用热敏电阻测量所实现的温控效果相当。研究结果为实现微型光学原子磁强计激光频率锁定、功率锁定以及气室温控提供了一种可行方案。

参 考 文 献

- [1] Allred J C, Lyman R N, Kornack T W, et al. High-sensitivity atomic magnetometer unaffected by spin-exchange relaxation[J]. Physical Review Letters, 2002, 89(13): 130801.
- [2] Preusser J, Knappe S, Kitching J, et al. A microfabricated photonic magnetometer[C] // 2009 IEEE International Frequency Control Symposium Joint with the 22nd European Frequency and Time forum, April 20-24, 2009, Besancon, France. New York: IEEE Press, 2009: 1180-1182.
- [3] 邵行来,薛春纪,严育通,等.地面高精度连续磁测在西天山群吉萨依铜矿勘查中的运用[J].新疆地质, 2011, 29(3): 342-347.
- [4] Shao X L, Xue C J, Yan Y T, et al. The significance of the near-continuous ground magnetic method and application to the prospecting for Qunjisai copper mine in the West Tianshan[J]. Xinjiang Geology, 2011, 29(3): 342-347.
- [5] Bulatowicz M, Larsen M. Compact atomic magnetometer for global navigation (NAV-CAM)[C] // Proceedings of the 2012 IEEE/ION Position, Location and Navigation Symposium, April 23-26, 2012, Myrtle Beach, SC, USA. New York: IEEE Press, 2012: 1088-1093.
- [6] Lu H S, Zhang J W, Li S D, et al. New concept submarine and related prospective technology[J]. Chinese Journal of Ship Research, 2008, 3(3): 77-80.
- [7] 郝杰鹏,周斌权.碱金属气室无机电加热技术研究与系统设计[J].计算机测量与控制, 2017, 25(5): 180-183.
- [8] Hao J P, Zhou B Q. Study on non-magnetic heating technology and system for alkali vapor cells[J]. Computer Measurement & Control, 2017, 25(5): 180-183.
- [9] 徐昆,曹进文,任秀艳,等.用于原子气室的温度控制系统、光泵磁力仪和核磁共振陀螺仪:CN209605833U[P]. 2019-11-08.
- [10] Xu K, Cao J W, Ren X Y, et al. Temperature control system for atomic gas chamber, optical pump magnetometer and nuclear magnetic resonance gyroscope: CN209605833U[P]. 2019-11-08.
- [11] Castro P, LeCun R, Manana M, et al. Infrared temperature measurement sensors of overhead power conductors[J]. Sensors, 2020, 20(24): 7126.
- [12] 刘帅,曾琦,黎超超,等.基于飞秒光纤光栅的准分布式高温传感器及应用[J].激光与光电子学进展, 2022, 59(1): 0106007.
- [13] Liu S, Zeng Q, Li C C, et al. Application of quasi-distributed high temperature sensor based on femtosecond fiber Bragg grating[J]. Laser & Optoelectronics Progress, 2022, 59(1): 0106007.
- [14] 王卓,刘祀浔,袁琪,等.一种基于外差干涉的气室温度控制系统:CN113776686A[P]. 2021-12-10.
- [15] Wang Z, Liu S X, Yuan Q, et al. Air chamber temperature control system based on heterodyne interference: CN113776686A [P]. 2021-12-10.
- [16] Alecock C B, Itkin V P, Horrigan M K. Vapour pressure equations for the metallic elements: 298-2500K[J]. Canadian Metallurgical Quarterly, 1984, 23(3): 309-313.
- [17] Seltzer S J. Developments in alkali-metal atomic magnetometry [D]. Princeton: Princeton University, 2008.
- [18] Allan D W. Statistics of atomic frequency standards[J]. Proceedings of the IEEE, 1966, 54(2): 221-230.
- [19] Yan Y G, Liu G, Lin H X, et al. VCSEL frequency stabilization for optically pumped magnetometers[J]. Chinese Optics Letters, 2021, 19(12): 121407.
- [20] 张继业,李雪,张建伟,等.垂直腔面发射激光器研究进展[J].发光学报, 2020, 41(12): 1443-1459.
- [21] Zhang J Y, Li X, Zhang J W, et al. Research progress of vertical-cavity surface-emitting laser[J]. Chinese Journal of Luminescence, 2020, 41(12): 1443-1459.

- [16] Schwindt P D D, Knappe S, Shah V, et al. Chip-scale atomic magnetometer[J]. Applied Physics Letters, 2004, 85(26): 6409-6411.
- [17] 刘畅, 肖垚, 刘恒, 等. 多结级联垂直腔面发射激光器失效分析[J]. 发光学报, 2022, 43(3): 388-395.
- Liu C, Xiao Y, Liu H, et al. Failure analysis of multi-junction cascade vertical cavity surface emitting laser[J]. Chinese Journal of Luminescence, 2022, 43(3): 388-395.

Cell Temperature Control Using Atomic Absorption Spectrum

Wu Lizhen^{1,2}, Zhu Xiaojie^{1,2}, Jiang Shuanghui^{1,2}, Tian Yuan¹, Zhang Yi^{1**}, Chen Jiehua^{1*}, Gu Sihong¹

¹Key Laboratory of Atomic Frequency Standard, Innovation Academy for Precision Measurement Science and Technology, Chinese Academy of Sciences, Wuhan 430074, Hubei, China;

²School of Physics, University of Chinese Academy of Sciences, Beijing 100049, China

Abstract

Objective Miniature optical atomic magnetometers are small, low-power, and highly sensitive. They have broad application prospects in geological exploration, geomagnetic navigation, and underwater target detection. To realize a miniature optical atomic magnetometer, it is necessary to accurately measure the temperature of the cell and achieve high-precision temperature control of the cell. In various existing temperature measurement methods, such as infrared, grating, and optical refractive index temperature measurements, the temperature measurement structure is complex and difficult to miniaturize. Therefore, in this study, a spectral absorption method is proposed to measure the internal temperature of the cell. After stabilizing the power and frequency of the incident light, the cell temperature is controlled by projecting the light from the cell. This method provides an alternative scheme for the temperature control of the cell of a miniature optical atomic magnetometer.

Methods In this study, the atomic absorption spectrum was used to measure the temperature of the cells. First, the feasibility of using the absorption spectrum to control temperature was theoretically analyzed. The theoretical analysis shows that when the incident laser intensity is locked and the laser frequency is locked at the center frequency of the spectral line, the light intensity transmitting the cell is only related to the temperature. Subsequently, an experimental platform was developed (Fig. 1). In the experimental setup, a laser was produced using a vertical-cavity surface-emitting laser (VCSEL). First, the laser output power was detected by a photodetector, and a laser power servo was applied to control the VCSEL-injection current, thus locking the optical power. Subsequently, the atomic absorption spectrum line was detected and converted to a laser frequency-discriminating signal by synchronous modulation and demodulation technology. A laser frequency servo was applied to control the laser temperature, consequently locking the laser frequency at the center of the absorption spectrum line. Finally, the signal amplitude at the center of the atomic absorption spectrum was used to measure the cell temperature and realize cell temperature control. We achieved cell-temperature control using this scheme. The temperature control scheme proposed in this paper and the temperature control realized using the thermistor 1 measurement were used, and thermistor 2 was used to evaluate the control effect.

Results and Discussions It was observed that when the laser intensity and frequency were locked, the laser noise power spectral density decreased in the low-frequency area (Fig. 2), and after locking, the light intensity before and after the cell decreased with the increase in cell temperature (Fig. 3). For our experimental parameters, the optimal working temperature of the cell for our scheme is 65–70 °C. A fitting curve was created using the theory, and the error of the cell temperature calculated by the fitting curve was not more than ± 0.3 °C within the range of 61–75 °C. The variation in temperature with time in the two control modes was recorded, as shown in Fig. 4(a). The Allan variance calculated according to Fig. 4(a) is shown in Fig. 4(b). It can be observed that the Allan variances for the two temperature control methods are almost equivalent, indicating that the temperature control effect is equivalent.

Because the laser intensity and frequency are locked, the produced laser can be easily employed to polarize the atoms. The assembly in the scheme is easily miniaturized, and this scheme is suitable for fabricating miniature atomic magnetometers. When applied to a miniature atomic magnetometer, the temperature sensitivity of the magnetometer can be reduced, and the performance of the magnetometer deteriorates slightly after long-term operation.

Conclusions In this study, we proposed a scheme to measure and control the temperature of a cell using the atomic absorption spectrum. We used this scheme to achieve laser power and frequency locking, as well as temperature control of the cell. After the laser power and frequency locking were realized, the laser intensity noise was reduced compared to the free-running state. We also used a thermistor to measure the temperature of the cell to realize the temperature control of the cell. The temperature control effect of the scheme proposed in this study is nearly equivalent to that achieved using a thermistor. This study provides a feasible scheme for realizing laser frequency locking, power locking, and cell temperature control of miniature optical atomic magnetometers.

Key words laser optics; miniature optical atomic magnetometer; cell temperature control; atomic absorption spectrum; laser frequency stabilization